Heliyon 8 (2022) e09501

Contents lists available at ScienceDirect

Heliyon

journal homepage: www.cell.com/heliyon

Research article

Inhibitory activity of xanthoangelol isolated from Ashitaba (*Angelica keiskei* Koidzumi) towards α-glucosidase and dipeptidyl peptidase-IV: *in silico* and *in vitro* studies

Diah Lia Aulifa [a,*], I Ketut Adnyana [b], Sukrasno Sukrasno [c], Jutti Levita [d]

[a] *Department of Pharmaceutical Analysis and Medicinal Chemistry, Faculty of Pharmacy, Universitas Padjadjaran, Sumedang, 45363, Indonesia*
[b] *Department of Pharmacology and Toxicology, School of Pharmacy, Bandung Institute of Technology, Bandung, 40132, Indonesia*
[c] *Pharmaceutical Biology Research Group, School of Pharmacy, Bandung Institute of Technology, Bandung, 40132, Indonesia*
[d] *Department of Pharmacology and Clinical Pharmacy, Faculty of Pharmacy, Universitas Padjadjaran, Sumedang, 45363, Indonesia*

ARTICLE INFO

Keywords:
Angelica keiskei
Xanthoangelol
α-glucosidase
Dipeptidyl peptidase-IV

ABSTRACT

In Indonesia, the sap *of Angelica keiskei* Koidzumi has been utilized traditionally as a blood-sugar reducer, nonetheless, its molecular mechanism still needs to be studied. This study aimed to isolate xanthoangelol (XA) from the yellow sap of *A. keiskei* planted in Mount Rinjani, Indonesia, and to investigate its mechanism by *in silico* and *in vitro* methods towards α-glucosidase and dipeptidyl peptidase-IV (DPP-IV). The dried yellow sap was macerated using ethanol, subjected to liquid-liquid extraction using a different polarity of solvents, further gradient-eluted with column chromatography. The isolated compound, formed as yellow crystals, melting point 114–114.4 °C, λ_{max} 368 nm, *m/z* 393.20 $[M + H]^+$, was confirmed as XA. Acarbose, an α-glucosidase inhibitor, and sitagliptin, a DPP-IV inhibitor, respectively, were employed as the reference drugs for both the *in silico* and *in vitro* studies. XA interacts with essential amino acid residues 232–237 in the *N*-terminal *N*-loop of α-glucosidase by forming a hydrogen bond with Ala234, a salt-bridge with Asp232, and 9 hydrophobic interactions (binding energy -7.81 kcal/mol; Ki = 1.99 μM). These binding modes resemble those of acarbose. Moreover, XA forms hydrogen bonds with Glu205 and Glu206 in the subsite S2 and π-π interaction with Phe357 in the extensive subsite S2 of DPP-IV (binding energy -8.34 kcal/mol; Ki = 0.873 μM), which are similar to those of sitagliptin. XA inhibits both α-glucosidase (IC_{50} XA = 14.45 μM; IC_{50} acarbose = 207 μM) and DPP-IV (IC_{50} XA = 10.49 μM; IC_{50} sitagliptin = 0.87 μM). Taken together, XA isolated from the yellow sap of *A. keiskei* Koidzumi might possess the potential to be further developed as an inhibitor of α-glucosidase and DPP-IV.

1. Introduction

Type 2 DM (T2DM) is one of the most common diabetes mellitus (DM) diseases in the last 10 years and will continue to increase in the next 10 years (Olokoba et al., 2012; Yang et al., 2019). T2DM is indicated by insulin insensitivity and failure of pancreatic beta cells to produce sufficient insulin (Saisho, 2015). This condition leads to a decrease in the transport of glucose to the liver, muscle cells, and fat cells (Siddiqui et al., 2013).

One of the anti-T2DM drugs that are widely used and work efficiently in delaying the absorption of carbohydrates from the small intestine thereby reducing blood glucose levels is the α-glucosidase inhibitor (AGI) (Mori et al., 2016; Rosak and Mertes, 2012; Siddiqui et al., 2013; Yang et al., 2019), such as acarbose, miglitol, and voglibose. Due to the side effects of these synthetic AGIs (flatulence, abdominal pain, and diarrhea), many studies have been carried out to explore new AGIs from plant sources as an alternative (Olokoba et al., 2012; Van de Laar, 2008). *A. keiskei* extract is known to reduce plasma glucose and insulin levels (Luo et al., 2012; Zhang et al., 2015).

Another mechanism anti-T2DM drugs is by regulating a group of metabolic hormones (incretin) that decelerate gastric emptying and suppress appetite (Mori et al., 2016). Incretins such as glucagon peptide-1 (GLP-1), and insulinotropic peptide (GIP) can maintain glucose homeostasis by stimulating insulin biosynthesis and inhibiting glucagon release (Charbonnel and Cariou, 2011). During food digestion, GLP-1 and GIP are released from the intestine in response to carbohydrate intake, yet these two incretins are rapidly halted by the DPP-IV enzyme (Nauck et al., 2011; Richter and Bandeira-echtler, 2008). The use of DPP-IV

* Corresponding author.
E-mail address: diah.lia@unpad.ac.id (D.L. Aulifa).

https://doi.org/10.1016/j.heliyon.2022.e09501
Received 24 February 2022; Received in revised form 11 April 2022; Accepted 16 May 2022

inhibitors avert the breakdown of GLP-1 and GIP, thereby increasing insulin production and suppressing glucagon production, both of which help lowering blood glucose levels thus, it would reduce the risk of complications on T2DM patient, such as obesity, heart disease, kidney and liver disorders (Avogaro and Fadini, 2014; Charbonnel and Cariou, 2011; Zilleßen et al., 2016).

One of the auspicious plants is *Angelica keiskei* Kodzumi (belongs to Apiaceae family). The yellow sap excreted from the stem and the root of the *A. keiskei* plant, is known to abundantly contain chalcones, e.g., xanthoangelols (XAs), 4-hydroxyderricin (4-HD) and isobavachalcone (Aulifa et al., 2020). Chalcones have been reported to be effective on maintaining glucose homeostasis (Wang et al., 2017). The ethanol extract of *A. keiskei* revealed a strong insulin-like activity pathway via peroxisome proliferator-activated receptor (PPAR-γ) activation, and effective for preventing insulin resistance (Enoki et al., 2007; Ohnogi et al., 2012). Zhang et al. (2015) reported that the ethyl acetate extract of *A. keiskei* could reduce the plasma glucose level, significantly attenuated increase in HOMA-IR and helped to retain the decreased adiponectin level on High fat-diet mice. Our previous study showed that ethanol extract of the leaves and the stem was not toxic to the human embryonic kidney (HEK293) cell line (Amalia et al., 2021). Moreover, *in vitro* study positively revealed that 4-HD, a chalcone compound isolated from the yellow sap of *A. keiskei*, inhibits DPP-IV (IC_{50} = 81.44 μM) weaker than that of sitagliptin (IC_{50} = 0.87 μM) (Aulifa et al., 2019). Albeit the reports on the anti-T2DM activity of chalcone isolated *A. keiskei* plant, no study was performed on the inhibitory activity of XA isolated from the yellow sap of *A. keiskei* towards DPP-IV and α-glucosidase. In this work, we isolated XA from the yellow sap of *A. keiskei* by employing column chromatography. Furthermore, we explored the inhibitory activity of this chalcone towards DPP-IV and α-glucosidase through *in silico* and *in vitro* studies.

2. Materials and methods

2.1. Plant materials

The stem (and the yellow sap taken from the stem) of *A. keiskei* was collected from Sembalun Village, Nusa Tenggara Barat, Indonesia. The plant was taxonomically identified by a certified biologist at the Herbarium Bandungense, Bandung Institute of Technology (ITB) (Document No. 401/I1.CO@.2/PL/2019). The yellow sap (1 L) was freeze-dried (2 × 24 h).

2.2. Chemicals

Human DPP-IV (Sigma-Aldrich, Cat. No. D4943), Gly-Pro-p-Nitroanilide Hydrochloride (GPPN) (Sigma-Aldrich, Cat. No. G0513), Tris-HCl Buffer (Sigma-Aldrich, Cat. No. T3253), α-glucosidase from *Saccharomyces cerevisiae* (Sigma-Aldrich, Cat. No. G5003), p-nitrophenyl-α-D-glucopyranoside (Sigma-Aldrich, Cat. No. N1377) and the other chemicals were purchased from Merck. Sitagliptin and acarbose, which used as reference drugs, were purchased from PT Kimia Farma Tbk., Indonesia, and PT Pharos Tbk., Indonesia, respectively.

2.3. Extraction and isolation

The leaves (100 g) and the stem (100 g) of *A. keiskei* were macerated with ethanol (1:6.5 w/v, triplicates), followed by evaporate the solvent. The yellow sap (750 mL) obtained from the stems of the *A. keiskei* plant was freeze-dried, yielded 31.59 g of yellow sap powder. The sap powder (10 g) was macerated with ethanol (1:5 w/v, triplicates), and then evaporated the solvent. Subsequently, the viscous extract was fractionated by liquid–liquid extraction three times by using three solvents, i.e., n-hexane, ethyl acetate, and water, then the obtained fractions were dried *in vacuo* (the yields were 4.3%, 58.6%, and 29%, respectively). All extracts were stored in closed containers at cool temperature for *in vitro* testing.

The isolation procedure for the sap *A. keiskei* was carried out on the ethyl acetate fraction by adapting our previous method of Aulifa et al. (2019), yielding 194.2 mg of isolated compound XA.

2.4. Characterization

XA, yellow crystals with melting point 114–114.4 °C. Characterization using an ultraviolet visible spectrophotometer (Agilent 845x UV Vis system) showed the maximum wavelength (λ) = 368 nm. The results of analysis using mass spectrometry (XevoTM QTOF MS, ionization mode ES $^{+)}$ yielded $[M + H]^+$ m/z = 393.20. Further analysis used ^{13}C-NMR (Agilent, 125 MHz) and ^{1}H-NMR (Agilent, 500 MHz). The data were compared with those of Kim et al. (2013); and presented in Table 1. Two-dimensional (2D) NMR was carried out with heteronuclear single quantum coherence (^{1}H, ^{13}C gHSQC) (Kawabata et al., 2011; Kim et al., 2013), which confirmed that $C_{25}H_{28}O_4$ was xanthoangelol (XA).

2.5. In silico study

In silico study comprises of the preparation of the ligands, the preparation of the macromolecules, and the molecular docking simulation.

2.5.1. Preparation of the ligands

The 2D structure of sitagliptin (Figure 1a), acarbose (Figure 1b), and XA (Figure 2) were prepared using ChemBioDraw Ultra 12.0 and ChemBio3D Ultra 12.0 (downloaded from www.cambridgesoft.com) programs. The 3D structure was geometry optimized using MM2 and AM1, and predicted its physicochemical properties (volume, number of hydrogen bond donors and acceptors).

2.5.2. Preparation of macromolecules

The macromolecules were the 3D crystal of α-glucosidase (PDB code: 3W37, resolution 1.7 Å complexed with acarbose, crystallized by Tagami et al., 2013), and DPP-IV (PDB code: 1X70, resolution 2.1 Å in complex with sitagliptin, crystallized by Kim et al., 2005), downloaded from the Protein Data Bank (PDB) (www.rcsb.org). The macromolecules were analyzed for the active site and its ligand interaction using Ligand Explorer Viewer 4.2.0. Subsequently, the macromolecules were separated from their natural ligands using SwissPDBViewer v.4.1.0 and the extracted ligands were employed to confirm the validity of the methods.

2.5.3. Validation of macromolecular molecular docking programs

Prior to the molecular docking simulation, the program was validated by re-docking the extracted ligand into its origin location (fifty times iterations) using Linux script command, subsequently the ligand was superimposed with the origin co-crystallized ligand. This step was continued by analyzing the root mean squared error (RMS error), calculating the standard deviation (SD) of the binding energy and inhibition constant (Ki).

2.5.4. Molecular docking simulation

Molecular docking simulation with 50x iterations was carried out on XA with DPP-IV and α-glucosidase. The molecular docking program used is Linux AutoDockVina (Trott and Olson, 2010) which has embedded MGLTools v.1.5.6, at position x 41.1841; y 51,045; z 35.6287, within 7 Å distance centered to the ligand position for the DPP-IV enzyme (1X70), and at the position x 0.108773; y -1.91698; z -23.0532, within 8 Å distance centered to the ligand position for the enzyme α-glucosidase (3W37), calculated by employing bind module in PLANTS 1.2.

2.5.5. Analysis of molecular docking results

The results of molecular docking were analyzed using AutoDockTools-1.5.6 and Biovia Discovery Studio 4.5 Visualizer

Table 1. ^{1}H-NMR and ^{13}C-NMR Spectroscopic data (δ value) for Xantoangelol (XA).

XA (Kim et al., 2013) (solvent $CDCl_3$)				XA (solvent $(CD_3)_2CO$))			
δ C (ppm)	δ H (ppm)	CH (HSQC)	Position	δ C (ppm)	δ H (ppm)	CH (HSQC)	Position
-	1.85	(3H, s, 3″-CH3)	3″	15.46	1.81	(3H, s, -CH3)	3″
-	1.59	(3H, s, 7″-CH3)	7″	16.87	1.55	(3H, s, -CH3)	7″
-	3.49	(1H, d, *J* = 7.1 Hz, 1″-H)	1″	21.40	3.41	(1H, d, *J* = 7.3 Hz, 1″-H)	1″
-	1.63	(3H, s, 8″-CH3)	8″	24.97	1.61	(3H, s, -CH3)	8″
-	2.10	(2H, m, 5″-H)	5″	26.55	2.06	(2H, m, -CH2)	5″
-	2.08	(2H, m, 4″-H)	4″	39.66	1.98	(2H, m, -CH2)	4″
-	6.43	(1H, d, *J* = 8.9 Hz, 5′-H)	5′	107.27	6.55	(1H, d, *J* = 8.9 Hz, 5′-H)	5′
-				113.51			3′
-	7.55	(2H, d, *J* = 8.5 Hz, 2,6-H)	2,6	115.91	6.94	(2H, d, *J* = 8.6 Hz, 2,6-H)	2,6
-	7.46	(1H, d, *J* = 15.4 Hz, α)	α	117.54	7.76	(1H, d, *J* = 16.1 Hz, α)	α
-	6.88	(2H, d, *J* = 8.5 Hz, 3,5-H)	3,5	130.81	7.72	(2H, d, *J* = 8.9 Hz, 3,5-H)	3,5
-	5.30	(1H, t, *J* = 7.1 Hz, 2″-H)	2″	122.35	5.32	(1H, t, *J* = 7.3 Hz, 2″-H),	2″
-	5.05	(1H, m, 6″-H)	6″	124.24	5.08	(1H, m, 6″-H)	6″
-				127.52			
-	13.88	(1H, s, 2′-OH)	2′		13.75	(1H, s, 2′-OH)	2′
-	7.72	(1H, d, *J* = 8.9 Hz, 6′-H)	6′	129.33	7.97	(1H, d, *J* = 8.9 Hz, 6′-H)	6′
-				131.50			1′
-				131.63			9″
-				135.41			10″
-	7.83	(1H, d, *J* = 15.4 Hz, β)	β	144.03	7.85	(1H, d, *J* = 15.4 Hz, β)	β
-				162.90			4′
-				162.72			4
-				165.14			2′
-				192.92		(C=O)	

Figure 1. 3D structure of sitagliptin (a); and acarbose (b) (downloaded from https://pubchem.ncbi.nlm.nih.gov/).

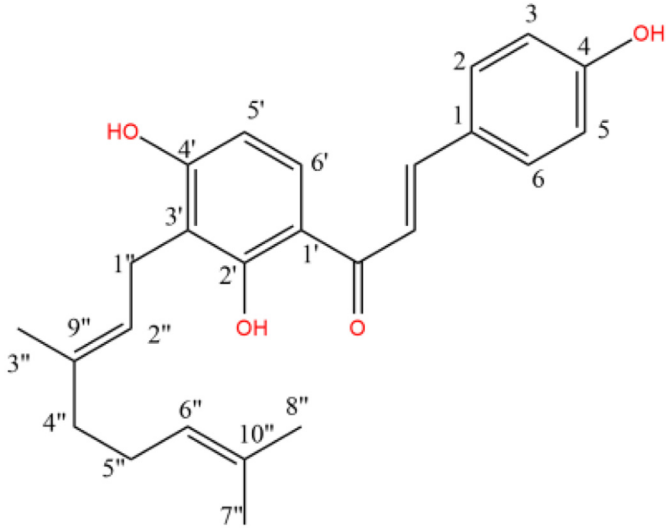

Figure 2. Structure of xanthoangelol (XA).

Table 2. The physicochemical properties of the ligands.

No.	Ligands	Volume (Å)	Hydrogen bond donor	Hydrogen bond acceptor
1	XA	1199.5	3	4
2	Acarbose	1519.5	14	20
3	Sitagliptin	1010.5	2	2

(downloaded from https://discover.3ds.com). Parameters observed were the binding mode, the binding energy, and the inhibition constant (Ki).

2.6. *In vitro study*

2.6.1. *Inhibition of α-glucosidase activity*

This study was carried out by following a previous method (Luo et al., 2012; Mayur et al., 2010) with slight modifications in 96 microwells plate. Test samples at various concentrations (3.125; 6.25; 12.5; 25; 50; and 100 ppm), 40 μL phosphate buffer 0.2 M (pH 7.0), 25 μL substrate p-nitrophenyl α-D-glucopyranose (PNPG), this reaction mixture was incubated at 37 °C for 10 min, then was added 25 μL of α-glucosidase enzyme solution (0.05 units/mL) and incubated again at 37 °C for 15

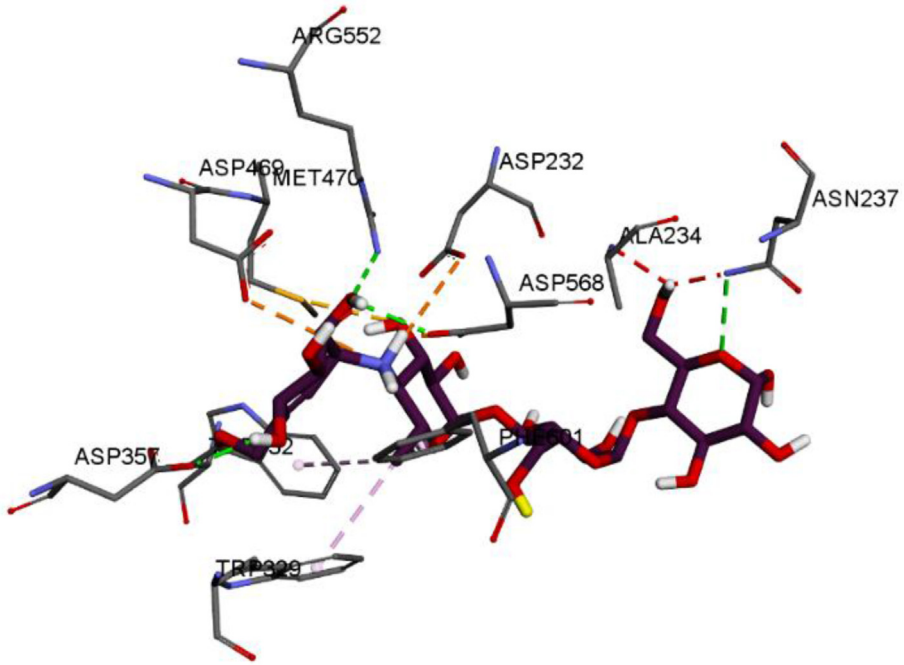

Figure 3. The binding mode of acarbose with α-glucosidase (Description: --- = salt bridge, --- = hydrogen bonding, --- = hydrophobic).

Figure 4. Superimposed structures of acarbose (RMSD = 1.024 Å).

min. The reaction was stopped by adding 100 μL of 0.2 M sodium carbonate solution (Luo et al., 2012; Mayur et al., 2010; Yang et al., 2012). Enzymatic hydrolysis of the substrate was monitored using Multiscan (Nanoquant, Infinite M2000 Pro, TECAN) at 405 nm, by counting the amount of p-nitrophenol released.

α-glucosidase enzyme solution (0.05 units/mL), 20 mM of 4-nitrophenyl β-D-glucuronide (PNPG) substrate, and 0.2 M phosphate buffer (pH 7.0) without the addition of inhibitor was used as the negative control. Acarbose was used as an inhibitor (positive control). All experiments were carried out in triplicates (n = 3). The inhibition percentage of α-glucosidase is obtained by the following formula:

$$\%\ \text{Inhibition} = \frac{(A - C) - (B - C)}{(A - C)} x100$$

Description:
A = absorbance of the negative control.
B = absorbance of the inhibitor with enzyme.
C = absorbance of the inhibitor without enzyme.

IC_{50} is calculated using a polynomial curve (Ramsay and Tipton, 2017). Using this equation, the concentration of the extract which inhibits the activity of α-glucosidase by 50% can be determined.

2.6.2. Inhibition of dipeptidyl peptidase-IV activity

Dipeptidyl peptidase-IV (DPP-IV) assay was conducted according to our previous research (Aulifa et al., 2019).

3. Results

The ^{1}H-NMR and ^{13}C-NMR spectrum of XA is presented in Table 1.

^{1}H-NMR (500 MHz, $(CD_3)2CO$): 1.81 (3H, s, 3″-CH_3); 1.55 (3H, s, 7″-CH_3); 3.41 (1H, d, J = 7.3 Hz, 1″-CH); 1.61 (3H, s, 8″-CH_3); 2.06 (2H, m, 5″-CH_2); 1.98 (2H, m, 4″-CH_2); 6.55 (1H, d, J = 8.9 Hz, 5′-CH); 6.94 (2H, d, J = 8.6 Hz, 2,6-CH); 7.76 (1H, d, J = 16.1 Hz, α); 7.72 (2H, d, J = 8.9 Hz, 3,5-CH); 5.32 (1H, t, J = 7.3 Hz, 2″-CH); 5.08 (1H, m, 6″-CH); 13.75 (1H, s, 2′-OH); 7.97 (1H, d, J = 8.9 Hz, 6′-CH); 7.85 (1H, d, J = 15.4 Hz, β). ^{13}C-NMR (125 MHz, $(CD_3)2CO$)): 15.46 (3″-C); 16.87 (7″-C); 21.40 (1″-C); 24.97 (8″-C); 26.55 (5″-C); 39.66 (4″-C); 107.27 (5′-C); 113.51; 115.91 (2,6-C); 117.54 (α-C); 130.81 (3,5-C); 122.35 (2″-C); 124.24 (6″-C); 127.52; 129.33 (6′-C); 131.50; 131.63; 135.41; 144.03 (β-C); 162.90; 162.72; 165.14; 192.92 (C=O).

Based on the gHSQC spectrum, the presence of three methyl groups, and two methylene groups were confirmed. The spectrum of eight quaternary carbons can be observed in the absence of correlation between the eight carbon signals (113.51; 131.50; 131.63; 135.41; 162.90; 162.72; 165.14). Additional signal at 5.07; 5.08; 5.09; 5.31; 5.32; 5.33; verified the presence of a geranyl group (two prenyl groups), and the signal at 192.92 validated a carbonyl group. The structure can be seen in Figure 2.

3.1. In silico study

The results of the computational prediction of the physicochemical properties of the ligands are presented in Table 2.

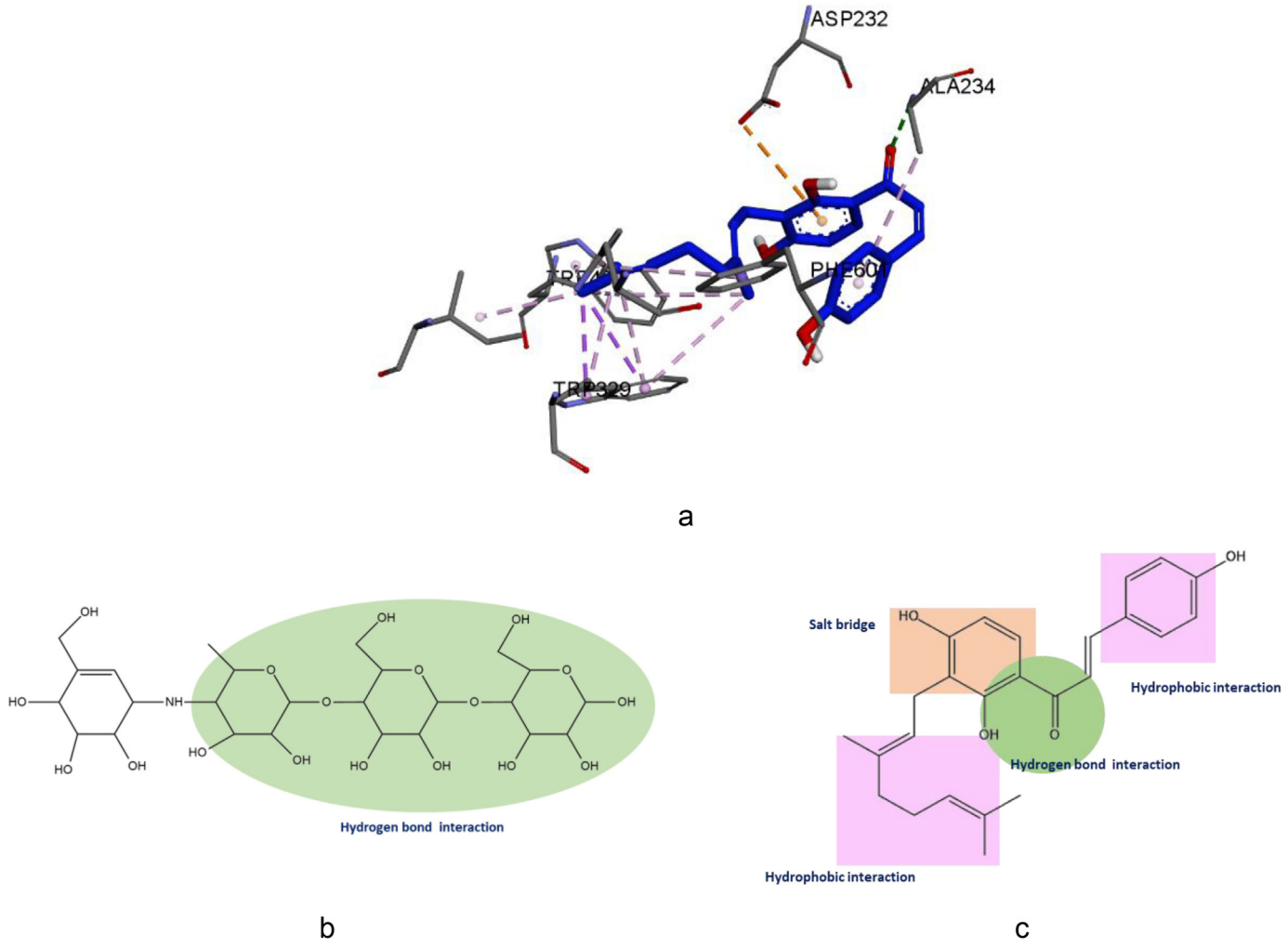

Figure 5. The binding mode of XA with α-glucosidase in 3D (a); common pharmacophore of acarbose (b) suggested by Tagami and coworkers (Tagami et al., 2013); and the proposed pharmacophores of XA (c) (Description: --- = salt bridge, --- = hydrogen bond, --- = hydrophobic).

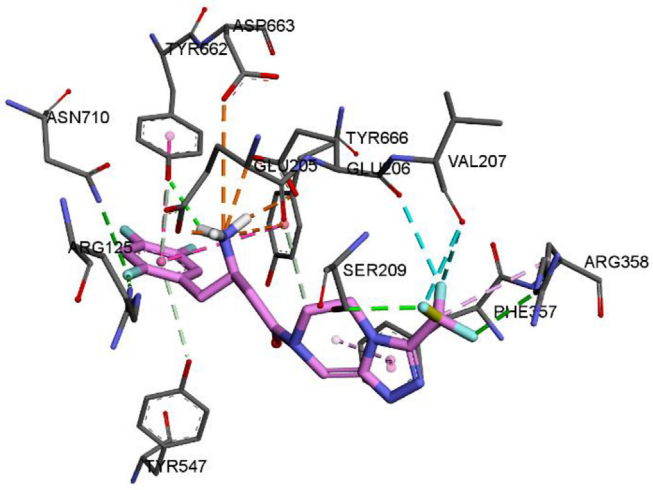

Figure 6. The binding mode of sitagliptin with DPP-IV (Description: --- = salt bridge, --- = hydrogen bond, --- = hydrophobic).

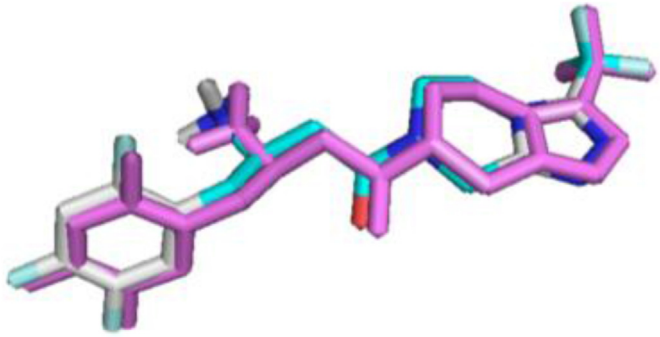

Figure 7. Superimposed structures of sitagliptin (RMSD 1.013 Å).

3.2. *Molecular docking simulation of XA towards α-glucosidase*

The active pocket of the α-glucosidase enzyme consists of important amino acid residues at position 232–237 in the *N*-terminal *N*-loop. These residues play a role in the biological activity of the enzyme (Tagami et al., 2013).

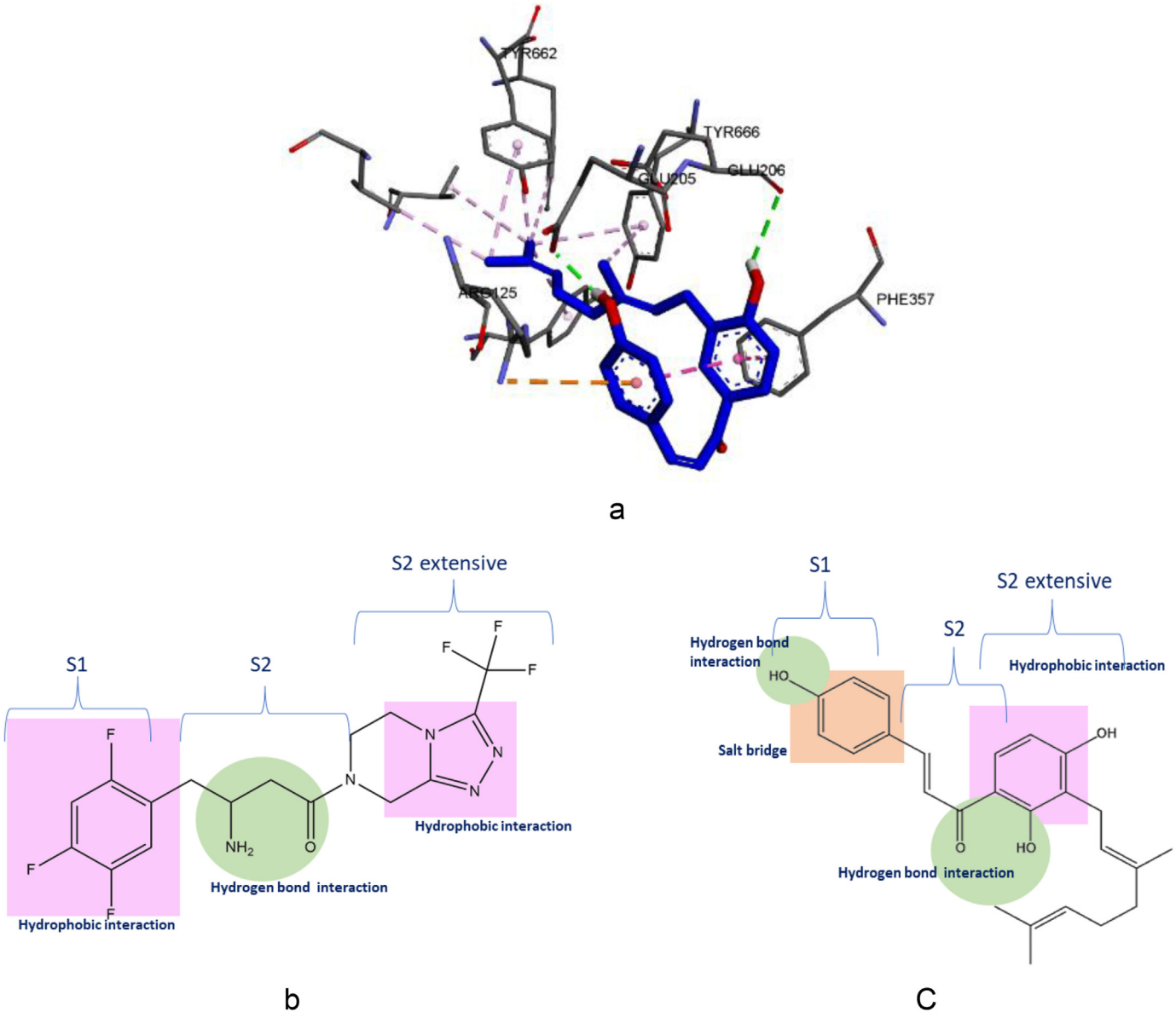

Figure 8. The binding mode of XA with DPP-IV in 3D (a); common pharmacophore of sitagliptin (b) suggested by previous workers (Arulmozhiraja et al., 2016; Nabeno et al., 2013); and the proposed pharmacophores of XA (c) (Description: --- = salt bridge, --- = hydrogen bond, --- = hydrophobic).

The re-docking of acarbose to α-glucosidase, crystallized by Tagami et al. from beet plant (Tagami et al., 2013), showed the formation of three hydrogen bonds with residues Asn237, Arg552, and Asp558. In addition, there were salt bridges with Asp232, Asn237, Trp239, Asp469, and Met470 (binding energy -7.81 kcal/mol; Ki = 2.14 μM) (Figure 3).

Moreover, the superimpose of two acarbose molecules produces an RMSD value of 1.024 Å (Figure 4), has confirmed the validity of the molecular docking simulation.

XA (Figure 5a) interacts with α-glucosidase through the formation of hydrogen bonds with Ala234 and salt bridges with Asp232, as well as 9 hydrophobic interactions (binding energy -7.81 kcal/mol; Ki = 1.99 μM).

3.3. Molecular docking simulation of XA towards DPP-IV

The re-docking of sitagliptin to its original location reveals interaction with Glu205 and Glu206 by forming a salt bridge, and hydrogen bonds with residues Ser209, Arg125, Arg358, Tyr662, and Asn710, as well as interactions with Phe357 through two aromatic interactions or π – π stackings (binding energy -9.24 kcal/mol; Ki = 0.172 M) as depicted in Figure 6.

The superimpose of two sitagliptin molecules produces an RMSD value of 1.013 Å (Figure 7) which confirmed the validity of the molecular docking simulation.

XA interacts with DPP-IV via two hydrogen bonds with Glu205 and Glu206, and π-π interaction with Phe357 on ring B (binding energy -8.34 kcal/mol; Ki = 0.873 μM) can be observed in Figure 8a. DPP-IV inhibitor compound which can bind to S1, S2, and S2 extensive subsites, tended to increase its inhibitory activity and its selectivity to related prolile peptidases (Nabeno et al., 2013). Interestingly, sitagliptin binds to the S1, S2, and S2 extensive subsites, it can be seen in Figure 8b which shows the concept of this categorization Class 3 (Figure 9).

The amino group of sitagliptin builds four hydrogen bonds, namely one hydrogen bond with the hydroxyl group of Tyr662, and three hydrogen bonds with the carboxylic oxygen of two glutamate residues (Glu205 and Glu206). It also interacts with Phe357 (strong hydrophobic interaction on S2 extensive) via two aromatic or π – π arrangements. *N*-terminal interactions are those that form salt bridges with Glu205 and

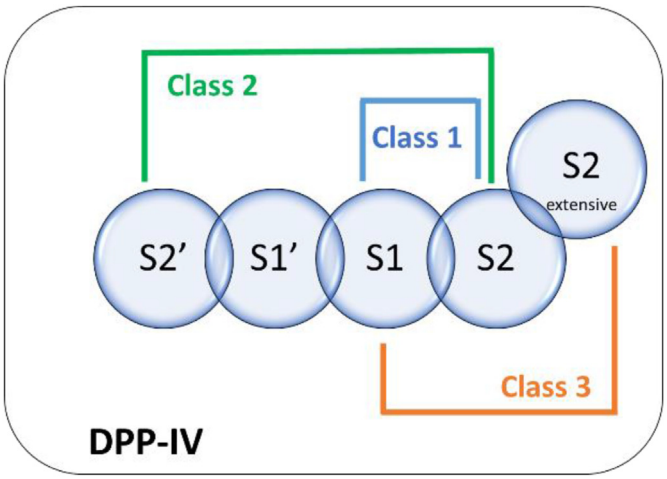

Figure 9. Concept of three classes of binding modes for DPP-IV inhibitors (modified from Nabeno et al., 2013).

Table 3. Inhibitory Activitiy of *A. keiskei* Extracts, Fractions, and XA toward α-glucosidase and DPP-IV enzymes.

Samples	α-glucosidase Enzyme (IC_{50})		DPP-IV Enzyme (IC_{50})	
	(μg/mL)	(μM)	(μg/mL)	(μM)
Ethanol extract of leaves	91.5	-	-	-
Ethanol extract of stems	117.7	-	-	-
Ethanol extract of yellow sap	16.76	-	5.94	-
Ethyl acetate fraction of yellow sap	20.38	-	34.03	-
XA	-	14.45	-	10.49
Acarbose	-	207	-	-
Sitagliptin	-	-	-	0.74

(Description: - = not tested).

Glu206 in the S2 subsite, both amino acid residues which play an important role in their inhibition of activity (Arulmozhiraja et al., 2016; Kim et al., 2005; Nabeno et al., 2013). Interesting fact, XA also has interaction in S2 extensive (Figure 8c).

3.4. *In vitro* inhibitory study of the plant extracts against DPP-IV and α-glucosidase

The *in vitro* inhibitory study of the plant extracts, fractions, and XA against these two enzymes is presented in Table 3.

All parts of *A. keiskei* plant inhibits α-glucosidase and DPP-IV, however, the ethanol extract of yellow sap shows the highest activity which is better than the standard. The inhibition of XA on DPP-IV indicates a strong activity with the IC_{50} = 10.49 μM. Furthermore, XA inhibits α-glucosidase with the IC_{50} = 14.45 μM better than that of acarbose (IC_{50} = 207 μM). It could be predicted that the XA compound may have antidiabetic activity through inhibition of α-glucosidase and DPP-IV.

4. Discussions

Our work revealed that XA, an alkylated chalcone, is found abundantly in the ethyl acetate fraction of the yellow sap of *A. keiskei* stems, as confirmed by the mass spectrometry and the ^{1}H and ^{13}C NMR. In flavonoid biosynthesis, chalcones are the precursors that possess an open C-ring and responsible for yellow pigment color in plant (Enoki et al., 2007; Mahapatra et al., 2015; Mayur et al., 2010). The carbonyl is relatively a strong dipole could act as a hydrogen bond acceptor (Zhuang et al., 2017). The presence of conjugated double bonds with the carbonyl group (C = O) is believed to be responsible for their pharmacological activity (Ramsay and Tipton, 2017; Salehi et al., 2021; Yang et al., 2012), as we proposed for XA in Figures 5c and 8c.

Acarbose, an α-glucosidase inhibitor, interacts with seven residues Asp232, Ala234, Asn237, Asp357, Arg552, Asp568, His626, through the formation of 14 hydrogen bonds in the active site at the *N*-loop. If there is an interaction at the *N*-terminal position on the *N*-loop band, the activity of the polysaccharide hydrolysis process into glucose will be inhibited (Tagami et al., 2013). Our molecular docking simulation exhibits that XA interacts with important residues at positions 232–237 on the *N*-terminal *N*-loop band (active site) α-glucosidase, similar to the interaction of acarbose (Figures 5b,c), therefore, XA might inhibit α-glucosidase.

DPP-IV, which expressed on the surface most cell types, is very specific serine protease (Makrilakis, 2019). This enzyme can recognizes amino acid sequences that have proline or alanine at the *N*-substrate peptide (*N*-terminal) end that deactivates or produces biologically active peptides (Arulmozhiraja et al., 2016; Nabeno et al., 2013). At the protease active site, the subsites are determined by the peptide binding site of the substrate. The amino acids in the substrate peptide categorized into three Class on their bunding site, and numbered from the cleavage point to the S2, S1, S1′, S2′, and S2 extensive subsites (Nabeno et al., 2013), as shown in Figure 9. Based on the molecular docking simulation, XA reveals interaction with residues Glu205 and Glu206 on the S2 subsite, and also with Phe357 residue on the S2 extensive subsite in the active site of the DPP-IV, which mimics the interaction of sitagliptin (Figures 8b,c), thus, XA might inhibit DPP-IV as well.

Inhibition of α-glucosidase leads to the blocking of carbohydrate breakdown in the digestive tract, thus eventually reducing the blood glucose level (Halegoua-De Marzio and Navarro, 2013), whereas inhibition of DPP-IV can prolong the lifelime of GLP1 and GIP in the intestine, which results in the stimulation of insulin secretion by β-pancreatic cells, and ultimately decreases blood glucose level (Deacon, 2011; Mahapatra et al., 2015; Makrilakis, 2019).

5. Conclusions

Xanthoangelol has been isolated in abundance in the ethyl acetate fraction of the yellow sap of *A. keiskei* stems. This isolation technique of this compound was performed by employing gravity column chromatography. Molecular docking simulation revealed that xanthoangelol interacts with important amino acid residues at positions 232–237 in the *N*-terminal *N*-loop of α-glucosidase, and important residues Glu205 and Glu206 on the S2 subsite, and Phe357 on the S2 extensive subsite of DPP-IV. These particular interactions bear resemblance to the inhibitors of α-glucosidase and DPP-IV. More interestingly, xanthoangelol strongly inhibits α-glucosidase and DPP-IV better the inhibitors of these enzymes. These findings suggest that xanthoangelol might possess antidiabetic activity through α-glucosidase and DPP-IV inhibition, therefore, this chalcone is potential to be further explored and developed.

6. Institutional review board statement

Not applicable.

7. Informed consent statement

Not applicable.

Declarations

Author contribution statement

Diah Lia Aulifa: Conceived and designed the experiment; Performed the experiments; Analyzed and interpreted the data; Contributed reagents, materials, analysis tools or data; Wrote the paper.

I Ketut Adnyana & Sukrasno Sukrasno: Conceived and designed the experiment; Analyzed and interpreted the data.

Jutti Levita: Conceived and designed the experiment; Analyzed and interpreted the data; Wrote the paper.

Funding statement

Dr. Diah Lia Aulifa was supported by Universitas Padjadjaran [4895/UN6.3.1/PT.00/2021].

Data availability statement

Data included in article/supp. material/referenced in article.

Declaration of interest's statement

The authors declare no conflict of interest.

Additional information

No additional information is available for this paper.

Acknowledgements

We would like to thank to PT. Pharos Tbk., Indonesia and PT. Kimia FarmaTbk., Indonesia for kindly providing acarbose and sitagliptin.

References

Amalia, R., Aulifa, D.L., Zain, D.N., Pebiansyah, A., Levita, J., 2021. The cytotoxicity and nephroprotective activity of the ethanol extracts of angelica keiskei Koidzumi stems and leaves against the NAPQI-induced human embryonic kidney (HEK293) cell line. Evidance-based complement. Alternative Med. 2021.

Arulmozhiraja, S., Matsuo, N., Ishitsubo, E., Okazaki, S., Shimano, H., Tokiwa, H., 2016. Comparative binding analysis of dipeptidyl peptidase IV (DPP-4) with antidiabetic drugs -an ab initio fragment molecular orbital study. PLoS One 11, 1–15.

Aulifa, D.L., Adnyana, I.K., Levita, J., Sukrasno, S., 2019. 4-Hydroxyderricin isolated from the sap of angelica keiskei Koidzumi: evaluation of its inhibitory activity towards dipeptidyl peptidase-IV. Sci. Pharm. 87, 3–12.

Aulifa, D.L., Adnyana, I.K., Sukrasno, Levita, J., 2020. Updates on 4-hydroxyderricin and xanthoangelol of angelica plants: extraction and pharmacological activities. Rasayan J. Chem. 13.

Avogaro, A., Fadini, G.P., 2014. The effects of dipeptidyl peptidase-4 inhibition on microvascular diabetes complications. Diabetes Care 37, 2884–2894.

Charbonnel, B., Cariou, B., 2011. Pharmacological management of type 2 diabetes: the potential of incretin-based therapies. Diabetes Obes. Metabol. 13, 99–117.

Deacon, C.F., 2011. Dipeptidyl peptidase-4 inhibitors in the treatment of type 2 diabetes: a comparative review. Diabetes Obes. Metabol. 13.

Enoki, T., Ohnogi, H., Nagamine, K., Kudo, Y., Sugiyama, K., Tanabe, M., Kobayashi, E., Sagawa, H., Kato, I., 2007. Antidiabetic activities of chalcones isolated from a Japanese herb, angelica keiskei. J. Agric. Food Chem. 55, 6013–6017.

Halegoua-De Marzio, D., Navarro, V.J., 2013. Alpha-glucosidase inhibitors. In: Drug-Induced Liver Disease, pp. 519–540.

Kawabata, K., Sawada, K., Ikeda, K., Fukuda, I., Kawasaki, K., Yamamoto, N., Ashida, H., 2011. Prenylated chalcones 4-hydroxyderricin and xanthoangelol stimulate glucose uptake in skeletal muscle cells by inducing GLUT4 translocation. Mol. Nutr. Food Res. 55, 467–475.

Kim, D., Wang, L., Beconi, M., Eiermann, G.J., Fisher, M.H., He, H., Hickey, G.J., Kowalchick, J.E., Leiting, B., Lyons, K., Marsilio, F., Mccann, M.E., Patel, R.A., Petrov, A., Scapin, G., Patel, S.B., Roy, R.S., Wu, J.K., Wyvratt, M.J., Zhang, B.B., Zhu, L., Thornberry, N.A., Weber, A.E., 2005. (2R)-4-Oxo-4-[3-(Trifluoromethyl)-5,6-dihydro[1,2,4]triazolo[4,3-a]pyrazin- 7(8H)-yl]-1-(2,4,5-trifluorophenyl)butan-2-amine: a potent, orally active dipeptidyl peptidase IV inhibitor for the treatment of type 2 diabetes. J. Med. Chem. 141, 141–151.

Kim, J.H., Son, Y.K., Kim, G.H., Hwang, K.H., 2013. Xanthoangelol and 4-hydroxyderricin are the major active principles of the inhibitory activities against monoamine oxidases on angelica keiskei K. Biomol. Ther. 21, 234–240.

Luo, L., Wang, R., Wang, X., Ma, Z., Li, N., 2012. Compounds from angelica keiskei with NQO1 induction, DPPH scavenging and α-glucosidase inhibitory activities. Food Chem. 131, 992–998.

Mahapatra, D.K., Asati, V., Bharti, S.K., 2015. Chalcones and their therapeutic targets for the management of diabetes: structural and pharmacological perspectives. Eur. J. Med. Chem. 92, 839–865.

Makrilakis, K., 2019. The role of dpp-4 inhibitors in the treatment algorithm of type 2 diabetes mellitus: when to select, what to expect. Int. J. Environ. Res. Publ. Health 16, 1–20.

Mayur, B., Sandesh, S., Shruti, S., Sung-yum, S., 2010. Antioxidant and alpha-glucosidase inhibitory properties of carpesium abrotanoides L. J. Med. Plants 4, 1547–1553.

Mori, A., Ueda, K., Lee, P., Oda, H., Ishioka, K., Arai, T., Sako, T., 2016. Effect of Acarbose, Sitagliptin and combination therapy on blood glucose, insulin, and incretin hormone concentrations in experimentally induced postprandial hyperglycemia of healthy cats. Res. Vet. Sci. 106, 131–134.

Nabeno, M., Akahoshi, F., Kishida, H., Miyaguchi, I., Tanaka, Y., Ishii, S., Kadowaki, T., 2013. A comparative study of the binding modes of recently launched dipeptidyl peptidase IV inhibitors in the active site. Biochem. Biophys. Res. Commun. 434, 191–196.

Nauck, M.A., Kemmeries, G., Holst, J.J., Meier, J.J., 2011. Rapid tachyphylaxis of the glucagon-like peptide 1-induced deceleration of gastric emptying in humans. Diabetes 60, 1561–1565.

Ohnogi, H., Hayami, S., Kudo, Y., Deguchi, S., Mizutani, S., Enoki, T., Tanimura, Y., Aoi, W., Naito, Y., Kato, I., Yoshikawa, T., 2012. Angelica keiskei extract improves insulin resistance and hypertriglyceridemia in rats fed a high-fructose drink. Biosci. Biotechnol. Biochem. 76, 928–932.

Olokoba, A.B., Obateru, O.A., Olokoba, L.B., 2012. Type 2 diabetes mellitus: a review of current trends. Oman Med. J. 27, 269–273.

Ramsay, R.R., Tipton, K.F., 2017. Assessment of enzyme inhibition: a review with examples from the development of monoamine oxidase and cholinesterase inhibitory drugs. Molecules 22.

Richter, B., Bandeira-echtler, E., 2008. Emerging role of dipeptidyl peptidase-4 inhibitors in the management of type 2 diabetes. Vasc. Health Risk Manag. 4, 753–768.

Rosak, C., Mertes, G., 2012. Critical evaluation of the role of acarbose in the treatment of diabetes: patient considerations. Diabetes Metab. Syndrome Obes. Targets Ther. 5, 357–367.

Saisho, Y., 2015. β-cell dysfunction: its critical role in prevention and management of type 2 diabetes. World J. Diabetes 6, 109.

Salehi, B., Quispe, C., Chamkhi, Imane, El Omari, Nasreddine, Balahbib, Abdelaali, Sharifi-Rad, Javad, Bouyahya, Abdelhakim, Akram, Muhammad, Iqbal, Mehwish, Oana Docea, Anca, Caruntu, Constantin, Leyva-Gómez, Gerardo, Dey, Abhijit, Martorell, Miquel, Daniela, Les, F., 2021. Pharmacological properties of chalcones: a review of preclinical including molecular mechanisms and clinical evidence. Front. Pharmacol. 11, 7762–7810.

Siddiqui, A.A., Siddiqui, S.A., Ahmad, S., Siddiqui, S., Ahsan, I., Sahu, K., 2013. Diabetes: mechanism, pathophysiology and management-A review. Int. J. Drug Dev. Res. 5, 1–23.

Tagami, T., Yamashita, K., Okuyama, M., Mori, H., Yao, M., Kimura, A., 2013. Molecular basis for the recognition of long-chain substrates by plant α-glucosidases. J. Biol. Chem. 288, 19296–19303.

Trott, O., Olson, A.J., 2010. Software news and update AutoDock vina: improving the speed and accuracy of docking with a new scoring function, efficient optimization, and multithreading. J. Comput. Chem. 31, 455–461.

Van de Laar, A., 2008. Alpha-glucosidase inhibitors in the early treatment of type 2 diabetes. Vasc. Health Risk Manag. 4, 1189–1195.

Wang, T. yang, Li, Q., Bi, K. shun, 2017. Bioactive flavonoids in medicinal plants: structure, activity and biological fate. Asian J. Pharm. Sci. 13, 12–23.

Yang, H.K., Lee, S.H., Shin, J., Choi, Y.H., Ahn, Y.B., Lee, B.W., Rhee, E.J., Min, K.W., Yoon, K.H., 2019. Acarbose add-on therapy in patients with type 2 diabetes mellitus with metformin and sitagliptin failure: a multicenter, randomized, double-blind, placebo-controlled study. Diabetes Metab. J. 43, 287–301.

Yang, Z., Wang, Y., Weng, Y., Zhang, Y., 2012. Bioassay-guided screening and isolation of α-glucosidase and tyrosinase inhibitors from leaves of Morus alba. Food Chem. 131.

Zhang, T., Yamashita, Y., Yasuda, M., Yamamoto, N., Ashida, H., 2015. Ashitaba (angelica keiskei) extract prevents adiposity in high-fat diet-fed C57bl/6 mice. Food Funct. 6, 134–144.

Zhuang, C., Zhang, Wen, Sheng, C., Zhang, Wannian, Xing, C., Miao, Z., 2017. Chalcone: a privileged structure in medicinal chemistry. Chem. Rev. 117.

Zilleßen, P., Celner, J., Kretschmann, A., Pfeifer, A., Racké, K., Mayer, P., 2016. Metabolic role of dipeptidyl peptidase 4 (DPP4) in primary human (pre)adipocytes. Sci. Rep. 6, 1–12.